PCCP

Accepted Manuscript

ROYAL SOCIETY OF CHEMISTRY

www.rsc.org/pccp

PCCP

ARTICLE

Probing Protein Adsorption on Nanoparticle Surface by Second Harmonic Light Scattering

The adsorption of proteins on gold nanoparticles Received 00th April 20xx,
Accepted 00th August 20xx

DOI: 10.1039/x0xx00000x

www.rsc.org/

A. Das,[a] A. Chakrabarti[b] and P. K. Das[*a]

A new application of second harmonic light scattering to probe protein physisorption on gold nanoparticle surface in aqueous buffer is reported. The free energies of adsorption, the number of protein molecules adsorbed on the surface and the binding affinity of a moderate size protein, alcohol dehydrogenase (ADH) and a small protein, insulin have been determined using the change in second harmonic scattered light signal as a function of binding . With four different size gold nanoparticles from 15-60 nm it is seen that the free energy change, the affinity constant and the number of protein molecules adsorbed on the surface increases with increase in size. The binding can be reversed by centrifugation and the protein molecules can be desorbed quantitatively. The application of this method in studying thermodynamic parameters of weakly interacting biomolecules with nanoparticles for nanoparticle based diagnostic and therapeutic formulations is stressed.

Introduction

The Nanoparticle based drugs and therapeutics have been suggested for many existing disease and human conditions in recent times.[1] The efficacy and potency of many protein and peptide based nanoparticle formulations are reported to be excellent compared to conventional formulations without the nanoparticle carrier.[2] However, during the passage of the nanoparticle to the target inside the body, they have to come in contact with many biomolecules including proteins in the blood stream and body fluid which may affect the composition of the nanoparticle-drug cocktail. The adsorption of biomoleculespresentin the body fluid on the surface of nanoparticles[3] can affect and alter the surface properties of the formulation[4] and may even displace the potent drug molecule from the surface[5] and render the formulation useless. Hence, a quantitative estimation of protein nanoparticle interaction is necessary in order to design and administer nanoparticle based therapeutics and diagnostic agents and control their biomedical function. In a recent report Haber and co-workers have used highly sensitive but nonspecific second harmonic light scattering to determine the binding constant and free energy of adsorption of a dye molecule, malachite green on 15 nm gold nanoparticle suspension in water.[6]Gan et al. measured kinetic and thermodynamic parameters of thiol activation on silver nanoparticle surface using the same technique.[7]Interaction of the dynamic electric field of the incident lighton the gold nanoparticle surfacecreates a large second order surface polarization leading to high intensity second harmonic light scattering.This was first recognised by Dadap et al.[8] and later seen experimentally by Vance et al.[9] The intensity of the SH scattered light from these plasmonic nanoparticles strongly depends on the size,[10] shape,[11] composition,[12] etc. indicating that the surface second order polarization can be manipulated by external means. The second harmonic light scattering (SHLS) efficiency is significantly enhanced when the fundamental or harmonic wavelengths are tuned close to their localized surface plasmon resonance.[13]This resonance enhanced SHLS has been widely used in sensing applications.[14] The analyte binding on the nanoparticle surface changes the SHS response which is monitored. Zhang et al. looked at the second harmonic light scattering from goat anti-human immunoglobulin coated gold nanoparticles in the presence of antigen leading to large increase in SH scattering intensity due to aggregation of gold nanoparticles.[15] Protein adsorption at interfaces have been reported in the literature[16]but no group has, thus far, reported the measurement of free energy of adsorption of a protein on the nanoparticle surface by harmonic light scattering.In this paper, we follow the decrease in the resonance enhanced SHS intensity of gold nanoparticles (Au-NPs) after protein binding to the surfaceand extract thermodynamic parameters from the measured SHLS signal decay.Theconventional techniques like centrifugation and subsequent separation, isothermal titration calorimetry (ITC), etc. do not work for weakly interacting protein-nanoparticle systems. In ITC, the concentration of the particles and proteins have to be sufficiently high for making a reliable

[a] Department of Inorganic and Physical Chemistry, Indian Institute of Science,Bangalore 560012, India.
[b] Crystallography & Molecular Biology Division,Saha Institute of Nuclear Physics, HBNI1/AF Bidhannagar, Kolkata 700064, India.
Electronic Supplementary Information (ESI) available: [Characterization and stability check of Au-NPs are available]. See DOI: 10.1039/x0xx00000x

measurement[17] at which aggregation of protein and nanoparticle is a major threat for introducing large error in the data.In this article, we have demonstrated that for studying free energy of interaction between low affinity proteins and nanoparticles, SHLS is ahighly reliable and sensitive technique.Two unrelated proteins, alcohol dehydrogenase (ADH) which is a medium size (84 kD) protein and insulin which is a small protein (6kD) have been used in our experiments to obtain quantitative information about their interaction with gold nanoparticles.We have seen from earlier studies that the interaction between ADH and insulin with Au-NPs is weak at neutral pH where both the protein and citrate capped Au-NPscarrynegative charges.[18,19] However, the initial repulsive forces between the negative charges could be overcome by the attractive noncovalentinteraction of gold with functional groups containing S and N atoms in proteins. Such opposing forces is likely to lead to weak binding of the protein on the nanoparticle surface. In this paper, we probe this physisorptionof protein on the nanoparticle surface more quantitatively by the SHLS technique.

Results and Discussion

The second harmonic light scattering from a spherical noble metal nanoparticle having a face centered cubic arrangement of metal atoms in the lattice is supposed to be zero in the electric dipole approximation.[20] Yet large second harmonic scattered light intensity has been detected from spherical gold, [9] copper [10] and silver [12] nanoparticles in solution. In the "small particle limit"[21] where the diameter of the particles is small compared to the wavelength of incident light, large SHS light is detected at the 90^0 scattering geometry which has been used throughout this work.

The quadratic dependence of the second order scattering signal on the input light intensity was verified and the results are summarized in Fig 1. The experimental data were fitted to equation (1) where $I_{2\omega}$and $I_{\omega}$are the intensities of the SHS and incident light, respectively. *A* is a proportionality constant and the exponent, n determines the nature of the process.

$$I_{2\omega} = A(I_{\omega})^n \quad (1)$$

Equation (1) can be rewrittena

$$\log I_{2\omega} = \log A + n \log I_{\omega} \quad (2)$$

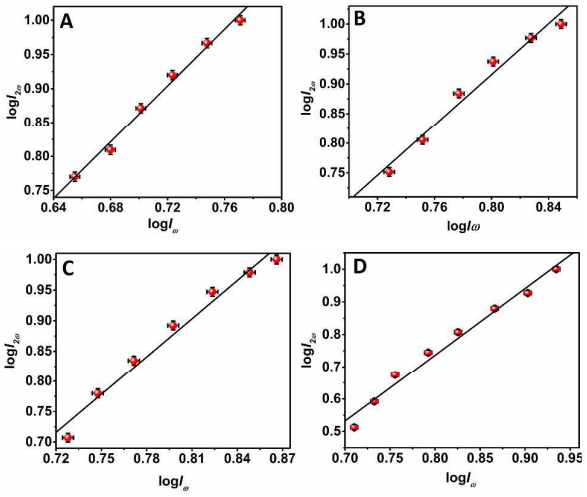

Fig 1. Normalized intensitiesof the SH and incident light are plotted in a log-log plot for A) 0.1 nM 15 nm Au-NPs , B) 0.032 nM 30 nm Au-NPs, C) 0.013 nM 45 nm Au-NPs, D) 0.008 nM 60 nm Au-NPs in 10 mM pH 7 phosphate buffer. The smooth lines through the experimental data points are fitted to equation (2) where the values of the exponent n obtained from the fitare A) 2.07 ± 0.10, B) 2.11 ± 0.17, and C) 2.08 ± 0.14, and D) 2.04 ± 0.12 , respectively.

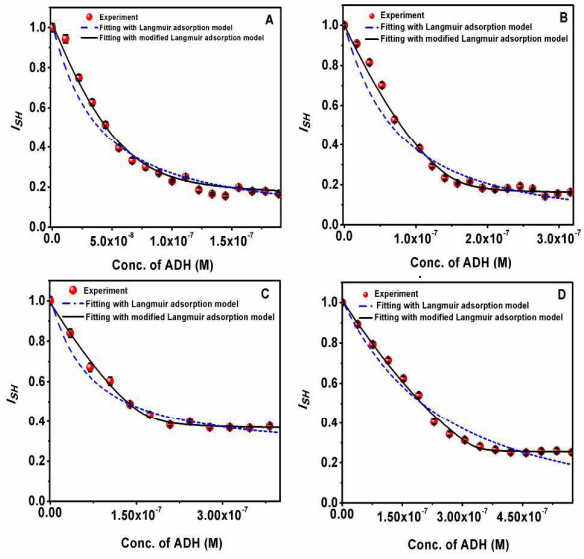

Fig 2. Normalized SH intensity at 532 nm from A) 0.1 nM 15 nm Au-NPs, B) 0.032 nM 30 nm Au-NPs, C) 0.013 nM 45 nm Au-NPs, D) 0.008 nM 60 nm Au-NPs at 10 mM pH 7 phosphate buffer as a function of addition of ADH. Each data points were recorded after ~ 1 min of ADH addition when the second harmonic signal became invariant with time. The SH intensity was normalized with respect to the SH intensity from pure Au-NP solution before addition of ADH.

Fig 2 shows that as small aliquots of the protein ADH are added to a fixed concentration of aqueous Au-NP dispersion in 10 mM pH 7 phosphate buffer at room temperature (298K), the second harmonic scattered light intensity decreases as a function of protein concentration.

With each addition of protein solution the decrease in the normalized SH intensity is significant (~5-10%) until it reaches a saturation point when no further decrease is seen. This reduction in SH signal is due to the adsorption of ADH on the surface of the Au-NPs. The surface polarization of citrate

capped Au-NPs as prepared is modified as the protein molecules dissolve in the solution and bind to the surface of the nanoparticles. At neutral pH in 10 mM phosphate buffer the Au-NPs are evenly dispersed in solution (see supplementary information) and the ADH molecules are negatively charged which was determined from the zeta potential measurement of the protein.[19] Therefore, the interaction between the NP surface and the protein is repulsive and not conducive for binding. However, ADH has twelvecysteine residues which containthiol groups and sulphur atomsare known to have affinity toward gold surface. This interaction of thiol groups with Au-NP surface helps ADH overcome the repulsive electrostatic forces and bind tothesurface resulting in a weak adsorption (physisorption). In fact, Gan et al.[7] reported that most of the SH signal generated from the surface of 80 nm citrate capped Ag-NPs can be quenched by adsorption of thiol molecules.The kinetics of interaction they proposed goes thorough physical adsorption, followed by a transition state to finally a chemical bond formation. In the transition state the old bonds of S with protons are weakened and S-Ag bonds begin to form.

The changes in the SHLS intensity can be quantitatively related to the protein coverage on the Au-NP surface and used for the determination of the free energy change of the adsorption process. This has been demonstrated for adsorption of small organic dyes on the micrometer sized polystyrene beads.[22]The adsorption isotherms for adsorption of ADH on different size Au-NPs are shown in Fig 2. In the Langmuir model of surface adsorption the surface is treated as a lattice of non-interacting sites and protein molecules from the bulk solution "react" with the empty surface sites resulting in binding. If the depletion of the bulk protein concentration due to adsorption is assumed to be miniscule and neglected compared to the bulk concentration, we obtain the usual expression for the Langmuir adsorption.

$$\frac{dN}{dt} = k_1 \frac{(C-N)}{55.5}(N_{max} - N) - k_{-1}N \qquad (3)$$

Where N is the number of adsorbed ADH molecules at the interface per unit volume, N_{max} is the maximum number of binding sites per unit volume, C is the total concentration of the protein molecules per unit volume and k_1 and k_{-1} are the rate constants for adsorption and desorption, respectively. The exchange of molecules between the bulk and the interface evolves according to k_1 and k_{-1}. After a while when equilibrium is established the rates of adsorption and desorption becomes equal and the equilibrium constant replaces the rate constants in equation (3) which can be recast as

$$\frac{N}{N_{max}} = \frac{1}{1+\frac{55.5}{KC}} \qquad (4)$$

Where N/N_{max} is nothing but the surface coverage, θ which influences the SH scattered signal, $I_{2\omega}$ from Au-NPs in solution. In writing equation(4) we have assumed that the number of adsorbed ADH molecules is very small compared to the bulk concentration of ADH and thus $(C-N) \approx C$. The normalized SH signal from Au-NPs is proportional to the concentration of the nanoparticles in solution.[11, 23]

$$\frac{I_{2\omega}}{I_\omega^2} = G\left(N_s\langle\beta_s^2\rangle + N_{Au-NP}\langle\beta_{Au-NP}^2\rangle\right) \qquad (5)$$

The SH signal from Au-NPs ($I_{2\omega}$) is normalized with the intensity of the input light (I_ω). $\langle\beta_s\rangle$and $\langle\beta_{Au-NP}\rangle$ are the orientation-averaged hyperpolarizability of the solvent and nanoparticles respectively. N_s and $N_{Au-NP}$are the number density of the solvent and nanoparticles, respectively. While writing equation (5) the hyperpolarizability of protein is neglected with respect to that of Au-NPs.From equation (5) it is seen that the normalized SH signal from Au-NPs is proportional to the number density of the nanoparticles, N_{Au-NP}, in solution. As the volume of the protein solution added per injection is very small compared to the total volume of the solution, the number density of the solvent and nanoparticles can be considered as remaining constant throughout the binding experiment. G is the proportionality constant which includes instrument factor, local field factor, etc. Adsorption of the protein molecules on the Au-NP surface causes the SH signal to decrease and the decrease is proportional toθ. Due to this adsorption process equation (5) can be written in the modified form as

$$I_{SH} = A\left|B - Q\theta e^{i\phi}\right|^2 \qquad (6)$$

Where I_{SH} is the normalized SH scattered light intensity, A is the proportionality constant which includes G, N_s, N_{Au-NP}, $\langle\beta_s^2\rangle$, etc., B is the 2nd order polarizability or 1st hyperpolarizability of citrate capped Au-NPs, Q is a factor which represents the signal that is quenched by the protein, and φ is the phase difference between the SH signal generated by the citrate capped gold surface and the surface after adsorption.

As we have detected incoherent second harmonic light in a fixed detection geometry of 90^0 the phase factor $e^{i\varphi}$ remains unchanged in all measurements and it can be absorbed within the Q factor and equation (6) is rewritten as

$$I_{SH} = \left|1 - Q'\vartheta\right|^2 \qquad (7)$$

Where we have absorbed the factor AB^2 in the normalization of $I_{SH}$and $Q' = Qe^{i\varphi}/B$. Now combining the Langmuir adsorption model and equation (7) we can write

$$I_{SH} = \left|1 - Q'\left(\frac{1}{1+\frac{55.5}{KC}}\right)\right|^2 \qquad (8)$$

The fit to the experimental data points in Fig 2 by equation (8) using a nonlinear least square fitting method with two parameters Q' and K is shown by blue lines. It is apparent that the fit is reasonable but not perfect. The data can be fitted better to a modified Langmuir adsorption model where the assumption that C is much greater than N is done away with.In fact, at low concentrations (micromolar) of ADH and with large

total surface area of the Au-NPs, in the modified Langmuir model, the surface coverage is expressed as

$$\theta = \frac{\left(C + N_{max} + \frac{55.5}{K}\right) - \sqrt{\left(C + N_{max} + \frac{55.5}{K}\right)^2 - 4CN_{max}}}{2N_{max}} \quad (9)$$

Hence, in the modified Langmuir model, the SH intensity is related to protein concentration as

$$I_{SH} = \left| 1 - Q' \left(\frac{\left(C + N_{max} + \frac{55.5}{K}\right) - \sqrt{\left(C + N_{max} + \frac{55.5}{K}\right)^2 - 4CN_{max}}}{2N_{max}} \right) \right|^2 \quad (10)$$

When equation (10) is fitted to the data in Figure 2, the modified Langmuir model gives a better fit. The values of K, N_{max} for the adsorption of ADH on the surface of Au-NPs obtained after fitting the modified Langmuir adsorption model have been listed in Table 1. The number of protein molecules adsorbed per nanoparticle at saturation (n_{sat}= N_{max}/$N_{Au\text{-}NP}$) is shown in Table 1. The Gibb's free energy for the binding of the protein on the surface sites can be calculated from the equilibrium constant using the thermodynamic equation ($\Delta G^0 = -RTlnK$). The values of the Gibb's free energy change for the adsorption of protein on the nanoparticle surface have been shown in Table 1.

Table 1. Thermodynamic parameters for the adsorption of ADH on Au-NPs surface. The protein and Au-NPs were dispersed in 10 mM pH 7 phosphate buffer at 25 ^{o}C.

Size of Au-NPs (nm)	Conc. of Au-NPs (nM)	N_{max} for ADH (X 10^{-8} M)	n_{sat} (X 10^2)	K (X 10^9)(M^{-1})	ΔG^0 (kJ/mol)
15	0.1	9.25 (± 0.12)	9.25 (± 0.12)	2.98 (± 1.18)	-54.0 (± 1.0)
30	0.032	15.13 (± 0.48)	47.27 (± 1.50)	10.97 (± 0.94)	-57.3 (± 0.2)
45	0.013	16.89 (± 0.93)	127.98 (± 7.04)	17.72 (± 3.24)	-58.5 (± 0.5)
60	0.008	33.29 (± 1.32)	416.11 (±16.5)	57.73 (± 8.92)	-61.4 (± 0.4)

The results indicate that the equilibrium mole ratio of ADH on Au-NPs (n_{sat}) increases with the size of Au-NPs. This is quite expected as the surface area of a nanoparticle increases with its size. It is seen from the table that the equilibrium constant and the free energy of binding, ΔG^0 increase monotonically with size which is counter-intuitive.

The fixed concentrations of the 15-60 nm Au-NPs employed in the adsorption experiments and shown in Table 1 have been chosen in such a way that the total surface area remain the same for different size Au-NPs in solution. This is to guarantee that the number of protein binding sites per unit surface area of the nanoparticles does not change from experiment to experiment. We find that the total number of protein molecules binding to the surface (N_{max}) increases with the size of the nanoparticles. What is the reason behind the increased affinity of protein on larger size nanoparticles? Is this due to the intrinsic difference in the nature of binding sites on different size nanoparticles? We think that this originates from the difference in protein packing on different curved surfaces. When protein molecules are bound to adjacent surface sites on a nanoparticle, protein-protein interaction enhances the binding. Since the surface curvature of bigger size nanoparticle is lower compared to smaller particles, the intermolecular end-to-end distance between the adjacent proteins will be larger in smaller particles leading to less close-packed arrangement and lower protein-protein interaction. On the other hand, on a flat surface the smaller intermolecular end-to-end distance between the adjacent proteins results in strong protein-protein interaction. This protein-protein interaction enhances the overall affinity of protein towards bigger size particles.

The basic assumption on which the Langmuir or modified Langmuir adsorption model is based is that the binding equilibrium is dynamic. For checking the reversibility of the binding, we have studied desorption of ADH from Au-NP surface. The detachment of ADH molecules from Au-NP surface was achieved by centrifugation of ADP-Au-NP conjugate at moderate speeds. The desorption of ADH from Au-NP surface was ascertained by steady-state fluorescence study and SHLS measurements.ADH contains a large numberof tryptophan residues which were excited at 280 nm and thefluorescence signal at 290-500 nm were recorded. The fluorescence signal from the supernatant, obtained after dislodging the protein from the nanoparticle-protein conjugate by centrifugation, was found to be almost similar in magnitude tothat obtained from pure ADH solution before addition to AuNps.This indicates almost complete desorption of ADH from nanoparticle surface by centrifugation rendering ADH in the supernatant and Au-NPs in the centrifugate. The presence of ADH in the supernatant was further verified by adding Au-NPs in the supernatant and measuring the SHLS intensity (see supplementary information). The desorption of ADH from Au-NP surface at moderate centrifugation speed (>5000rpm) indicates that the interaction between ADH and Au-NPs is indeed weak. In fact, from the analysis of the interaction of ADH with Au-NPs using modified Langmuir adsorption model,

it is revealed that ADH binds to the Au-NP surface by weak forces as the free energy change, ΔG^0 is of the order of -50 kJ mol^{-1}.[24] This explains the easiness of desorbing ADH from Au-NP surface and ADH is physisorbed on Au-NP surface.

In order to test if the SHLS technique is applicable to all physisorbed nanoparticle protein binding, the interaction of Au-NPs with another smaller protein (6 kD), insulin unrelated to ADH has been studied. The experimental data and the fitted adsorption isotherms of insulin binding to Au-NP surface using the modified Langmuir model are shown in Figure 3.

The values of K, N_{max}, ΔG^0 obtained after non-linear least square fitting of the experimental data(Figure 3)are listed in

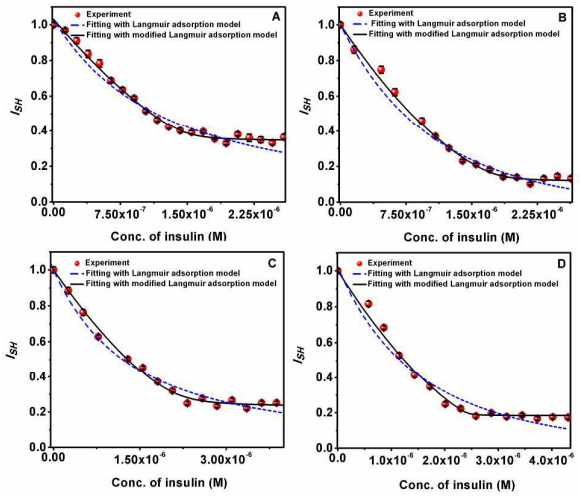

Fig 3. Normalized SH intensity at 532 nm from A) 0.1 nM 15 nm Au-NPs, B) 0.032 nM 30 nm Au-NPs, C) 0.013 nM 45 nm Au-NPs at 10 mM pH 7 phosphate buffer recorded as a function of concentration of insulin solution in 10 mM pH 7 phosphate buffer. Each data points were recorded after ~ 1 min of insulin addition. The SH intensity was normalized w.r.t. the SH intensity of Au-NPs solution before addition of insulin.

Table 2. In the table we have also shown the number of protein molecules adsorbed per nanoparticle at saturation (n_{sat}).

The trend observed for the thermodynamic quantities for the interaction of insulin with different size Au-NPs was the same as that of ADH. This reveals that these two proteins bind to the Au-NP surface by physisorption processes and the free energy change, ΔG^0 is of the order of 50 kJ mol^{-1}. Comparing the N_{max} in Tables 1 and 2 it is observed that the molar ratio of insulin adsorbed on a particular size Au-NP is greater than that of ADH. This is much expected as the size of insulin is smaller (molecular radius ~ 1.3 nm)[25, 26] than ADH (molecular radius ~ 3.5 nm)[27] and thus for a fixed surface area the number of molecules of insulin bound to the surface is larger than that of ADH.

Like ADH, desorption of insulin from Au-NP surface during the centrifugation process has been studied in a similar fashion using steady-state fluorescence and SHLS measurement.Insulin

Table 2. Thermodynamic parameters for the adsorption of insulin on Au-NPs. The protein and Au-NPs were dispersed in 10 mM pH 7 phosphate buffer at 25 °C.

Size of Au-NPs (nm)	Conc. of Au-NPs (nM)	N_{max} for insulin (X 10^{-6} M)	n_{sat} (X 10^4)	K (X 10^9)(M^{-1})	ΔG^0 (kJ/mol)
15	0.1	1.32 (± 0.21)	1.32 (± 0.21)	1.10 (± 0.98)	-51.6 (± 3.5)
30	0.032	1.73 (± 0.06)	5.41 (± 0.19)	2.84 (± 1.06)	-53.9 (± 1.0)
45	0.013	2.29 (± 0.04)	17.61 (± 0.31)	10.33 (± 2.83)	-57.1 (± 0.7)
60	0.008	2.43 (± 0.07)	30.37 (± 0.87)	25.29 (± 4.20)	-59.3 (± 0.4)

has also been found to be detachable from the Au-NP surface by centrifugation and the intrinsic fluorescence is recovered fully (see supplementary information).

The adsorption of protein on gold nanoparticles and the subsequent protein nanparticle conjugate are expected to be affected by the protein state, that are, the number of layers of protein, their packing on the surface, etc. From our earlier study[19] we have seen that the function of the protein remains more or less unaffected by the protein state in the protein nanoparticle conjugate. The thermodynamic quantities derived here are based on the monolayer model of Langmuir. However a modified Langmuir model was necessary to fit the experimental data better which perhaps indicates a multilayer formation on the surface. A more detailed study is necessary to ascertain this.

Experimental

Materials

$HAuCl_4.3H_2O$, insulin from porcine pancreas, and ADH from equine liver or yeast were purchased from Sigma-Aldrich and were used without further purification. Ascorbic acid, tri-sodium citrate (TSC), NaOH, potassium dihydrogen phosphate and dipotassium hydrogen phosphate were all obtained locally.

Synthesis of Au-NPs

The synthesis of 15-60 nm Au-NPs were accomplished by following a seed mediated growth method described by Ziegler and co-workers[28] after incorporating certain modifications. The details of the synthesis have been given in the supplementary information.

The concentration of the Au-NPs and consequently the molar extinction coefficients were determined from the total amount of precursor $HAuCl_4.3H_2O$ used in the synthesis and from the diameter of the Au-NPs following the method reported by Liu et al.[29]The Au-NPs were purified by centrifugation and the concentration after purification was determined using the molar extinction coefficient as determined earlier.

Characterization of morphology and stability of Au-NPs in phosphate buffer

The morphology of the Au-NPs was obtained from bright field transmission electron microscopy images. Bright field transmission electron micrographs of freshly prepared Au-NPs were taken in JEOL 100CXII transmission electron microscope (TEM) with 100 kV accelerating voltage. Sample preparation was done by drop coating Au-NPs solution on formvar carbon film on 200 mesh copper grids.The statistical distribution of size was obtained from the histogram of *ca* 500 particles (see Figure S1, supplementary information).

The absorption spectra of Au-NPs dispersed in solution was recorded in a Perkin-elmer Lambda-750 UV-Vis spectrophotometer in the wavelength range 200-800 nm with a slit- width of 2 nm (Figure S2, supplementary information).

Spectra of Au-NPs

The stability of the Au-NPs in phosphate buffer of pH 7.0 with different phosphate concentrations was studied by monitoring thew peak position and width ofthe surface plasmon absorption band (Figure S3, supplementary information). The results were further verified from the transmission electron microscope images (Figures S4 and S5, supplementary information). The results of SPR peak position and broadening of the spectra in phosphate buffer were compared with results in Au-NPs in milli-Q water and the stability of the AuNps in 10 mM phosphate buffer was confirmed. The stability of Au-NPs in buffer with time was checked by monitoring the SPR peak position and broadening of the UV-Vis spectra (Figure S6 supplementary information).

Second harmonic light scattering experiments

The second harmonic generation measurements for the adsorption of proteins on the surface of Au-NPs were done following a set-up similar to reported by L. H. Haber and co-workers with a few changes.[6]A Q-switched solid state Nd:YAG laser that delivers a fundamental beam of 1064 nm at a repetition rate of 10 Hz with a pulse width of 10 ns was used as the incident light source in the SHLS experiments. The fundamental laser beam with high peak power was guided by a couple of high energy laser mirrors and passed through a long pass colored glass filter before being focused into the sample. The sample solutions were taken in a cylindrical glass cell of diameter 2.5 cm and volume ~ 20 cc. The fundamental beam was focused by a plano-convex lens to a point 2-3 cm before the sample cell. The scattered SH photons from the sample were collected at 90° with respect to the incident beam propagation direction, at a large solid angle using a large diameter aspherical lens. The Rayleigh scattering and other stray light were cut down by a broad band IR filter followed by a 532 nm interference filter. The SH scattered signal was collected on a UV-Visible PMT and averaged typically over 512 shots in a digital storage oscilloscope and stored in a PC. During the SHS titrations of Au-NPs with proteins, the input laser energy was kept below 5 mJ/pulse in order to avoid degradation of protein molecules.Since both single photon and two photon fluorescence, in principle, can interfere with the SHLS signal in solution,a wavelength scan of the signal over 450-600 nm was performed by placing a monochromator (JobinYvon TRIAX 550) in between the filter and the PMT. A power dependence check with the spectrally resolved SH scattered signal yielded values similar to that displayed in Fig. 1. Since the filter set up is very sensitive and we can do the measurements at very low concentrations and laser intensities, the monochromator was removed from the experimental set-up after the quality check (Figure S7 in supplementary information).

Desorption of proteins by centrifugation

Solutions containing protein of concentration 0.23 mg/mL for ADH or 0.3 mg/mL for insulin in the absence and presence of different concentrations of Au-NPs in 10 mM pH 7 phosphate buffer were prepared and kept for ~ 5 min for equilibrium. The intrinsic fluorescence signal from protein in the range of 290-500 nm was found to quench with concentration of Au-NPs as a result of FRET from adsorbed proteins to Au-NPs. The results are shown and discussed in our earlier work.[19] The solutions of protein with and without Au-NPs are subjected to centrifugation for 30 min at a speed of 15000 rpm for 15 nm Au-NPs, 9000 rpm for 30 nm Au-NPs, 6000 rpm for 45 nm Au-NPs and approximately 5000 rpm for 60 nm Au-NPs. After centrifugation the supernatant was collected and analyzed using steady-state fluorescence from proteins. The intrinsic fluorescence of the protein after centrifugation in the supernatant was recorded and compared to that from the pure protein solution.Thefluorescence was recorded in the Horiba JobinYvon Fluoromax-4 Spectrofluorometer. The intrinsicfluorophoreswere excited at 280 nm and the emission was monitored in the range of 290-500 nm.[30]The excitation and emission band passes were kept at 5 nm. The results for desorption of ADH and insulin from Au-NP surface by centrifugation (Figures S8-S11 in supplementary information) show that the protein nanoparticle binding is indeed weak.

The details of the experimental procedure for studying centrifugation induced desorption of ADH and insulin from Au-NP surface probed via SHLS from Au-NPs have been given in supplementary information. The results are shown in Figures S12 and S13 in supplementary information.

Conclusions

SHG from the surface of Au-NPs has been used for the first time for the quantification of protein adsorption on a nanoparticle surface. The adsorption isotherm of two unrelated proteins, ADH and insulin adsorbed on different size Au-NP surface in aqueous buffer has been obtained by

following the second harmonic scattered light intensity as a function of bulk protein concentration at a fixed concentration of the nanoparticles. The experimental data fitted to a modified Langmuir adsorption isotherm yields the free energy of adsorption and the number of protein molecules adsorbed on the nanoparticle surface. Both proteins are physisorbed on the surface with a free energy of adsorption of ca. 50 kJ mol^{-1}, which points out that the interaction is, indeed, weak. The number of protein molecules adsorbed on the nanoparticle surface depends on the size of the particle as well as that of the protein. Although the free energy of adsorption of the small protein insulin and the moderate size protein, ADH is close, a specific Au-NP adsorbs more insulin molecules than ADH on their surface. More importantly, we found that the binding affinity of the protein depends on the size of the Au-NP and increases with increasing size. This is understood in terms of protein packing on a relatively flat surface for large size particles compared to that on a curved surface for small size particles where the protein-protein interaction will be minimal.

This promising SHG probe provides a powerful spectroscopic method for the determination of equilibrium adsorption parameters even for weakly interacting proteins with nanoparticles, which cannot be probed by conventional techniques at such low concentrations without introducing large errors. Since our Au-NPs are citrate capped and negatively charged and the proteins are also negatively charged at the neutral pH of the experiments, the surface charge effects will also affect the adsorption process and these need to be investigated further. Now-a-days biotechnology application of Au-NP based diagnostic and therapeutic formulations is gaining grounds and the quantitative information on biomolecule-nanoparticle interaction will be necessary to fine tune these formulations. Our investigation presented in this paper will perhaps open up the scope of many weakly interacting nano-bio systems by the SH light scattering technique in the near future.

Acknowledgements

PKD thanks the Ministry of Communication and Information Technology for the Centre of Excellence in Nanoelectronics, Phase II grant for generous funding of this work.

References

1 M. E. Davis,*Mol. Pharmaceutics,* 2009, **6**, 659;C-M. J.Hu, S. Aryal, L. Zhang, *Therapeutic Delivery,* 2010, **1**, 323; C. Spuch,O.Saida, C.Navarro,*Recent Pat. Drug Delivery Formulation,* 2012, **6**, 2; S. Dhar, W. L. Daniel, D. a. Giljohann, C.a. Mirkin, S. J.Lippard, *J. Am. Chem. Soc.,*2009, **131**, 14652; S. Sinha, D. K. Paul, R.Kanchanapally, A.Pramanik, S. R.Chavva, B. P. V. Nellore, S. J. Jones, P. C.Ray,*Chem. Sci.,* 2015, **6**, 2411;

2 E. C. Dreaden, S. C.Mwakwari, Q. H.Sodji, A. K.Oyelere, M. A. El-Sayed, *Bioconjug. Chem.,* 2009, **20**, 2247; J. Zhou, T. R. Patel, R. W. Sirianni,G.Strohbehn, M. Q. Zheng, N. Duong, T.Schafbauer, A. J.Huttner, Y. Huang, R. E. Carson, Y. Zhang, D. J.Jr. Sullivan, J. M.Piepmeier, W. M.Saltzman,*Proc. Natl. Acad. Sci. U.S.A.,* 2013, **110**, 11751;

3 S. H. D. P. Lacerda, J. J. Park, C. Meuse, D.Pristinski, M. L. Becker, A. Karim, J. F. Douglas, *ACS Nano,* 2010, **4**, 365; E. Casals, T.Pfaller, A.Duschl, G. J.Oostingh, V. Puntes, *ACS Nano,* 2010, **4**, 3623;

4 Y. K. Lee, E.-J. Choi, T. J. Webster, S.-H. Kim, D.Khang,*International Journal of Nanomedicine,* 2015, **10**, 97;

5 V. Voliani, G.Signore, R.Nifosi, F. Ricci, S.Luin, F.Beltram, *Recent Patents on Nanomedicine,*2012**,2,** 1;

6 L. H. Haber, S. J. J. Kwok, M.Semeraro, K. B.Eisenthal, *Chem. Phys. Lett.*, 2011, **507**, 11;

7 W. Gan, B. Xu, H.-L. Dai, *Angew. Chem. Int. Ed.,* 2011, **50**, 6622;

8 J. I. Dadap, J. Shan, T. F. Heinz, *J. Opt. Soc. Am. B*, 2004, **21**, 1328;

9 F. W. Vance, B. I. Lemon, J. T.Hupp, *J. Phys. Chem. B,* 1998, **102**, 10091;

10 M. Chandra, S. S. Indi, P. K. Das, *J. Phys. Chem. C,*2007, **111**, 10652;

11 A. Singh, A.Lehoux, H.Remita, J.Zyss, I.Ledoux-Rak, *J. Phys. Chem. Lett.,* 2013, **4**, 3958;

12 E. C. Hao, G. C. Schatz, R. C. Johnson, J. T.Hupp,*J. Chem. Phys.,* 2002, **117**, 5963;

13 M. Chandra, P. K. Das, *Chem. Phys. Lett.,* 2009, **476**, 62;

14 J. Duboisset, I.Russier-Antoine, E.Benichou, G. Bachelier, C. Jonin, P. F. Brevet, *J. Phys. Chem. C,* 2009, **113**, 13477; J. Butet, I. Russier-Antoine, C.Jonin, N.Lascoux, E. Benichou, P.-F. Brevet, *NanoLett*., 2012, **12**, 1697;

15 C. X. Zhang, Y. Zhang, X. Wang, Z. M. Tang, Z. H. Lu, *Anal. Biochem.,* 2003, **320**, 136;

16 S. W. H. Eijt, M. M. Wittebrood, M. A. C. Devillers, Th. Rasing, *Langmuir*, 1994, **10**, 4498;J. Rinuy, P. F. Brevet, H. H. Girault, *Biophys. J*., 1999, **77**, 3350;J. S. Salafsky, K. B. Eisenthal, *J. Phys. Chem. B* 2000, **104**, 7752-7755;

17 W. B. Turnbull, A. H. Daranas, *J. Am. Chem. Soc.,*2003, **125**, 14859; A. Gourishankar, S. Shukla, K. N. Ganesh, M.Sastry, *J. Am. Chem. Soc.,*2004, **126**, 13186;

18 P. K. Das, presented in part at the 246th ACS National Meeting, Fall, Indianapolis, September, 2013;

19 A. Das, A.Chakrabarti, P. K. Das, *RSC Adv.,* 2015, **5**, 38558;

20 G. S. Agarwal, S. S.Jha,*Solid State Commun*., 1982, **41**, 499; X. M. Hua, J. I.Gersten, *Phys. Rev. B,* 1986, **3***3*, 3756;

21 M. Chandra, P. K. Das, *Chem. Phys*., 2009, **358**, 203;

22 H. Wang, E. C. Y. Yan, L. Liu, K. B. Eisenthal, *J. Phys. Chem. B,* 1998, **102**, 4446;

23 K. Clays,A.Persoons, *Phys. Rev. Lett*., 1991, **66**, 2980;

24 P. D. Húmpola, H. S. Odetti, A. E. Fertitta, J. L. Vicente, *J. Chil. Chem. Soc.,* 2013, **58**, 1541;

25 P. R. Shorten, C. D. McMahon, T. K.Soboleva, *Biophysical journal,*2007, **93**, 3001;

26 A. Burkhardt, M. Warmer, S. Panneerselvam, A. Wagner, A. Zouni, C. Glöckner, R. Reimer, H. Hohenberg, A. Meents, *ActaCrystallogr Sect F StructBiolCrystCommun.*, 2012, **68***,* 495;

27 C. Vallet-Stkouve, L. Rat, J. M. Sala-Trepat, *Eur. J. Biochem*. 1976, **66**, 327;

28 C. Ziegler, A.Eychmüller, *J. Phys. Chem. C,*2011**, 115***,* 4502;

29 X. Liu, M. Atwater, J. Wang, Q.Huo, *Colloids and Surfaces B: Biointerfaces,*2007, **58**, 3;

30 P. L. Luisi, R. Favilla, *Eur. J. Biochem.* 1970, **17**, 91; N. L. Vekshin, *Biochemistry (Moscow),*2008, **73**, 458;

Graphical abstract